Article

# Enhanced Double Metal Cyanide Catalysts for Modulating the Rheological Properties of Poly(propylene carbonate) Polyols by Modifying Carbonate Contents

Harin Kim, Hyo-Jeong Lee, Jiwon Hwang, Su Min Jung, Jun Dong Park, and Joon Hyun Baik*

Read Online

ACCESS | Metrics & More | Article Recommendations | SI Supporting Information

**ABSTRACT:** Poly(propylene carbonate) (PPC) polyol is an environmentally sustainable material derived from abundant and renewable greenhouse gas, $CO_2$. Optimizing their synthesis and properties is crucial to their application in the production of polyurethane products. In this study, we synthesized PPC polyols with varying carbonate contents using heterogeneous Zn/Co double metal cyanide (DMC) catalysts, which were prepared with poly(ethylene glycol)-*block*-poly(propylene glycol)-*block*-poly-(ethylene glycol) (P123) as an effective complexing agent. Analysis of the influence of calcination temperature revealed that the DMC-P123 catalyst calcined at 100 °C exhibited superior catalytic performance owing to reduced crystallinity and enhanced formation of the monoclinic phase. Additionally, by precisely controlling the $CO_2$ pressure, high propylene carbonate contents of up to 32.8 wt % in the polyol structure were achieved. The increased carbonate content enhanced the intermolecular attraction between polyol chains, thereby promoting hydrogen bonding and significantly modulating the rheological properties of the polyol. The novel findings of this study establish a solid foundation for the synthesis of $CO_2$-based polyols with desirable properties, serving as alternatives to conventional petroleum-based polyols.
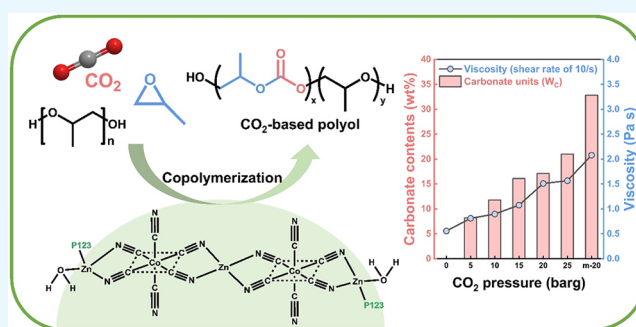
## INTRODUCTION

Carbon dioxide ($CO_2$) is a well-known greenhouse gas that contributes to global warming. However, its nontoxic nature, abundance, nonflammability, and cost-effectiveness have sparked interest in its potential as a renewable C1 feedstock for the environmentally friendly production of value-added chemicals.[1] An intriguing application is the direct utilization of $CO_2$ as a monomer or comonomer in polymerization reactions, offering advantages such as reduced production costs by replacing expensive raw materials and addressing the market demand for polymers.[2]

Polyols, which contain two or more hydroxyl groups per molecule, are crucial to the production of polyurethane (PU) products, including flexible and rigid foams, coatings, adhesives, sealants, and elastomers.[3,4] Depending on their specific application, they can be classified into polyether, polyester, and polycarbonate (PC) polyols. PC and poly-(propylene carbonate) (PPC) polyols are produced through the copolymerization of epoxides and $CO_2$ using different catalysts such as Co(III) complexes, Cr(III) complexes, or Lewis acids for the former and double metal cyanide (DMC) catalysts for the latter.[5] PC polyols have disadvantages such as a high glass transition temperature ($T_g$) and high viscosity at ambient temperature, making them unsuitable for preparing polyurethane foams.[2,6] In contrast, PPC polyols have a lower

$T_g$ and lower viscosity.[7] They also have a narrower molecular weight distribution (i.e., lower polydispersity index (PDI)) and lower levels of unsaturation than PC polyols.[8]

DMC catalysts have an exceptional capability for $CO_2$ insertion into the polyol structure. They are synthesized via the reaction of a metal salt (zinc chloride) with a metal cyanide potassium salt (potassium hexacyanocobaltate) in aqueous solution, resulting in a compound with a typical formula of $Zn_3[Co(CN)_6]_2 \cdot xZnCl_2 \cdot yH_2O$.[1] To enhance catalytic activity and ensure amorphous characteristics, a complexing agent such as an ester, alcohol, or surfactant is added to the synthesis mixture.[9−12] Notably, DMC catalysts exhibit negligible catalytic activity in the copolymerization of PO and $CO_2$ without a complexing agent.[9,13,14]

The present study reveals two significant developments in the synthesis and use of $CO_2$-based polyols. First, the calcination temperature of the DMC catalysts was optimized to explore its impact on the catalytic efficiency during the

copolymerization of PO and $CO_2$. Second, the rheological analysis of the polyols for their carbonate contents was conducted. Despite the numerous studies on synthesizing $CO_2$-based polyols using DMC catalysts, these specific findings have not been investigated previously. The calcination temperature affects the degree of oxidation and crystallinity of the metal ions, consequently influencing the activity, selectivity, and stability of the catalyst. Therefore, the optimization of the DMC catalysts can be achieved by manipulating the calcination temperature during their preparation. Because the catalytic copolymerization of PO and $CO_2$ is typically conducted at elevated temperatures (approximately 115−130 °C), selecting the appropriate calcination temperature for the DMC catalyst is crucial. Lower reaction temperatures result in insufficient catalyst activation, while higher temperatures can lead to the thermal decomposition of the polymer, compromising catalyst stability and selectivity.[13,15,16] Hence, this study determined the catalytic performance of DMC catalysts prepared at different calcination temperatures. To simplify the catalyst preparation method while achieving high catalytic performance, only the Pluronic P123 (P123) was used as the complexing agent, unlike in previous studies,[6,12,17,18] which also employed cocomplexing agents.

On the other hand, despite the widespread application of polyols in the synthesis of polyurethane products, there is no research focused on the rheological properties of $CO_2$-based polyols, particularly PPC polyols. Previous studies have predominantly explored various aspects of polyol synthesis or characterization.[8−10,19] Understanding how PPC polyols respond to different flow and deformation conditions can provide valuable insights into their processability and suitability for diverse polyurethane applications, including foams, coatings, adhesives, and elastomers. Rheological analysis of $CO_2$-based polyols enables manufacturers to fine-tune production processes, minimize waste, and increase efficiency.[20] Specifically, it ensures the optimum manufacturing quality and consistency of PU products. As no prior research has specifically conducted a rheological analysis of $CO_2$-based polyols, this study investigated the structural and rheological properties of $CO_2$-based polyols with varying carbonate contents. This essential information will contribute to a better understanding of the potential impact of the properties of $CO_2$-based polyols on PU manufacturing, which is instrumental in designing a system for efficient PU synthesis.

## ■ EXPERIMENTAL SECTION

**Materials.** All reagents were used as received. Chemicals, including zinc chloride ($ZnCl_2$, > 98%), potassium hexacyanocobaltate(III) ($K_3[Co(CN)_6]$, > 97%), poly-(ethylene glycol)-*block*-poly(propylene glycol)-*block*-poly-(ethylene glycol) (P123, $M_n$ ∼ 1100 g/mol), toluene (>99.8%), and (±)-propylene oxide (PO, ≥ 99%) were purchased from Sigma-Aldrich. Poly(propylene glycol) (PPG-1000, $M_n$ ∼ 1000 g/mol) was provided by Kumho Petrochemical Co., Korea.

**Preparation of DMC-P123 Catalysts.** DMC-P123 catalysts were prepared by using $ZnCl_2$ as a metal salt, $K_3[Co(CN)_6]$ as a metal cyanide salt, and P123 as a complexing agent as follows. Solution 1 was prepared by dissolving 13.63 g of $ZnCl_2$ and 1.1 g of P123 in 54 mL of distilled water. Solution 2 was prepared by dissolving 1.33 g of $K_3[Co(CN)_6]$ in 18 mL of deionized water. Solutions 1 and 2

were mixed and stirred together for 1 h at 50 °C. Subsequently, 1.1 g of P123 was added, and the mixture was stirred for an additional 5 min at the same temperature. The mixture was centrifuged several times with deionized water to remove unreacted ions and then calcined in a muffle furnace at various temperatures ranging from 60 to 200 °C. The calcined samples were designated as DMC-P123-$T$, where $T$ represents the calcination temperature (in °C). To elucidate the effect of the complexing agent, we prepared DMC-Pure by reacting $ZnCl_2$ with $K_3[Co(CN)_6]$ in an aqueous solution at 50 °C in the absence of P123. It was then centrifuged several times and calcined at 80 °C.

**Copolymerization of PO and $CO_2$.** As illustrated in Scheme 1, The copolymerization of PO and $CO_2$ was

**Scheme 1. Copolymerization Reaction of PO and $CO_2$ with an Initiator to Produce PPC Polyol**
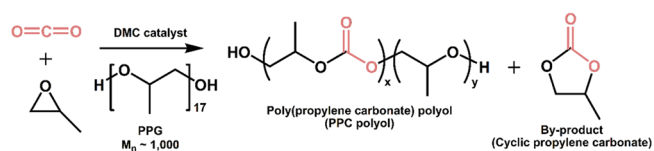


conducted in a 450 mL high-pressure reactor (Parr 4560, Parr Instrument Co.) using PPG-1000 as an initiator, in a similar manner to our previous work.[6] The reactor was charged with 150 mL of toluene as a solvent for the suspension of the catalyst, 30 g of PPG-1000, and a DMC-P123 catalyst (1000 ppm). The reactor was then purged with $CO_2$ several times to replace the air. The mixture was pressurized with $CO_2$ at pressures ranging from 5 to 25 barg (bar gauge). After heating the reactor to 115 °C with vigorous agitation, 116.16 g (2 mol) of the PO monomer was slowly added to the reactor over 90 min using a high-performance liquid chromatography (HPLC) pump. The system temperature was maintained at 115 °C for another 30 min to complete the polymerization. Toluene was removed by rotary evaporation, and the residue was washed with deionized water and chloroform to remove the cyclic propylene carbonate (cPC) produced as a byproduct. The catalysts employed in this study were not separated from the polyols due to their small quantity, and these catalysts typically have a negligible impact on polyurethane synthesis. The resulting products were denoted as PPC polyol-$x$, where $x$ is the weight percent of propylene carbonate units ($W_C$) calculated using eq 1 (vide infra).

**Characterization.** The metal contents of the catalysts were measured by inductively coupled plasma atomic emission spectroscopy (ICP-AES; Optima 8300 DV, PerkinElmer). The surface areas of the catalysts were determined based on the Brunauer−Emmett−Teller (BET) theory of the physical adsorption of nitrogen using a Tristar II 3020 surface area and porosity analyzer (Micromeritics). Powder X-ray diffraction (XRD) patterns were recorded by using a D8 Advance X-ray diffractometer (Bruker) with Cu Kα radiation. X-ray photoelectron spectroscopy (XPS) analysis was conducted using a Nexsa G2 spectrometer (Thermo Fisher Scientific) equipped with a monochromatic Al Kα radiation source operating at 12 kV and 10 mA. Thermogravimetric analysis (TGA) was performed using a TGA 4000 thermogravimetric analyzer (PerkinElmer) to investigate the thermal decomposition of the catalysts. The test temperature ranged from 40

to 600 °C at a heating rate of 10 °C/min under an air atmosphere. Fourier-transform infrared (FT-IR) spectra were recorded by using a Nicolet iS20 FT-IR spectrometer (Thermo Fisher Scientific). Scanning electron microscopy (SEM) images were obtained by using a JSM-7600F microscope (JEOL). The average molecular weight and PDI of PPC polyols were measured by gel permeation chromatography (GPC) using a 1260 HPLC system (Agilent) with Mixed-B and Mixed-E columns at 40 °C in tetrahydrofuran (HPLC grade). Measurements were conducted at a flow rate of 1 mL/min by using a polystyrene standard for calibration. The viscosities of PPC polyols were determined using a cone–plate geometry in an HR 20 rheometer (TA Instruments) by fixing the shear rate at 10/s and raising the temperature from 10 to 80 °C at a rate of 4 °C/min. $^1H$ NMR spectra were obtained by using an Avance III 500 MHz NMR spectrometer (Bruker) with deuterated chloroform ($CDCl_3$) as the solvent. For the copolymerization of PO and $CO_2$, the weight percent of propylene carbonate units ($W_C$) in PPC polyols was determined based on the integrated peak areas of $CH_3$ in the ether linkages ($A_{1.22}$) and carbonate units ($A_{1.35}$) using eq 1.[1,6,10] The weight percent of the cPC byproduct ($W_{PC}$) was determined based on the integrated peak area of $CH_3$ ($A_{1.5}$) using eq 2.[21,22]

$$W_C = 102A_{1.35}/(58A_{1.22} + 102A_{1.35})100 \quad (1)$$

$$W_{PC} = 102A_{1.5}/[58A_{1.22} + 102(A_{1.35} + A_{1.5})]100 \quad (2)$$

## ■ RESULTS AND DISCUSSION

**Optimizing the Calcination Temperature of the DMC Catalyst.** To evaluate the catalytic performance of the DMC-P123 catalysts calcined at different temperatures, copolymerization reactions of PO and $CO_2$ were conducted using these catalysts under the same reaction conditions (20 barg $CO_2$ pressure injection) (Table 1). There were no significant differences in the molecular weight, $W_C$, or $W_{PC}$ of the products except when DMC-P123−200 was used. In this case, the molecular weight and $W_C$ decreased and the polyol productivity was significantly lower. DMC-P123−200 showed very low activity, as evidenced by the high reactor pressure, even after copolymerization was complete (Figure 1). Thus, employing high calcination temperatures (e.g., above 150 °C) in the preparation of a catalyst for PO and $CO_2$ copolymerization is not conducive to achieving optimal catalytic activity. The DMC-P123 catalyst calcined at 100 °C exhibited the shortest induction period and fastest polymerization rate, as shown in Figure 1. Based on the polyol productivity (Table 1), a calcination temperature of 100 °C is recommended for obtaining a highly active DMC catalyst for PO and $CO_2$ copolymerization. When an identical set of experiments was performed using newly prepared batches of the DMC-P123-60, -100, and -200 catalysts, the polymerization activity exhibited a high degree of reproducibility, as depicted in Figure S1. This indicates that the catalyst preparation method and reactor system employed in this study are well-suited for the copolymerization of PO and $CO_2$.

Figure 2A illustrates the powder XRD patterns of the DMC catalysts calcined at various temperatures. The reference catalyst synthesized without a complexing agent, DMC-Pure, exhibited six distinct diffraction peaks at $2\theta$ = 15.0°, 17.4°, 24.7°, 35.2°, 39.5°, and 43.4°, indicating high crystallinity and indexing to the cubic space group $Fm3m$.[23,24] However, the

**Table 1. Catalytic Activity of DMC-P123 Catalysts Prepared at Different Calcination Temperatures in the Synthesis of PPC Polyols**[a]

| catalyst[b] | polyol productivity (g/g_cat)[c] | mol wt (g/mol) | | PDI[d] | $W_C$[e] (wt %) | $W_{PC}$[f] (wt %) |
| --- | --- | --- | --- | --- | --- | --- |
| | | $M_n$ | $M_w$ | | | |
| DMC-P123−60[g] | 864.9 | 3747 | 8767 | 2.3 | 19.8 | 11.3 |
| DMC-P123−80 | 928.0 | 3632 | 8510 | 2.3 | 17.4 | 11.0 |
| DMC-P123−100[g] | 936.1 | 3978 | 8448 | 2.1 | 20.6 | 11.5 |
| DMC-P123−150 | 906.3 | 3399 | 9038 | 2.7 | 19.9 | 10.0 |
| DMC-P123−200[g] | 226.3 | 1135 | 2640 | 2.3 | 3.9 | 4.8 |

[a]Reaction conditions: catalyst = 1000 ppm of feed, toluene = 150 g, $P_{CO_2}$ = 20 barg, reaction temperature = 115 °C, and reaction time = 2 h. [b]DMC-P123-$T$, where $T$ is the calcination temperature. [c]Values obtained after byproduct removal. [d]Determined by GPC relative to a polystyrene standard in THF. [e]Weight percent of propylene carbonate units in PPC polyol calculated using eq 1. [f]Weight percent of cyclic propylene carbonate in the product calculated using eq 2. [g]Average value of three experiments for reproducibility
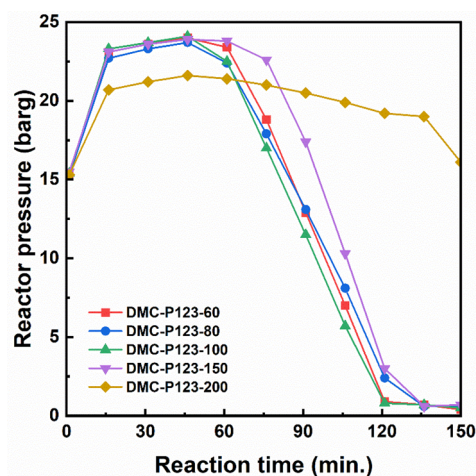


**Figure 1.** Change in reactor pressure during the copolymerization of PO and $CO_2$ using DMC-P123 catalysts calcined at different temperatures.

DMC-P123 catalysts prepared with an organic ligand complexing agent showed broader peaks and significantly lower crystallinity than DMC-Pure.[25] Furthermore, they exhibited new characteristic peaks at $2\theta$ = 16.0°, 19.3°, and 23.7°, suggesting the formation of monoclinic crystals and grain refinement.[26] This transformation of the crystalline structure from a cubic to an amorphous phase can be attributed to the coordination of bulky organic ligands to $Zn^{2+}$.[27] Notably, the DMC-P123-100 catalyst calcined at 100 °C exhibited the highest intensity of the peak at 23.7°, indicating the monoclinic phase of the DMC-P123 catalyst. Furthermore, the intensity of this peak decreased with increasing calcination temperature above 100 °C, at which point the peak at 17.4°, representing the cubic crystal, became prominent. Generally, enhancing the
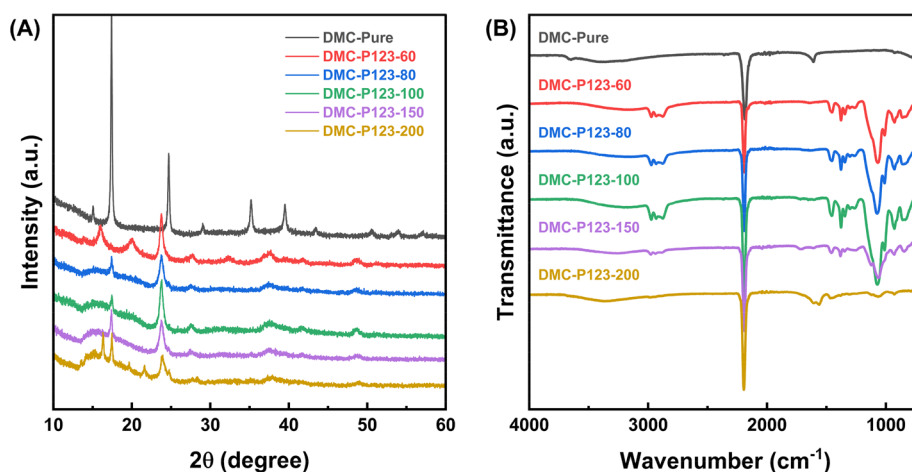
**Figure 2.** (A) XRD patterns and (B) FT-IR spectra of the DMC catalysts calcined at different temperatures.

formation of a monoclinic structure of the DMC catalyst influences its activity in polymerization reactions.[12,28] Therefore, the optimal calcination temperature of the catalyst should be determined to obtain a favorable structure for the copolymerization reactions.

The influence of calcination temperature on catalyst morphology was also observed through SEM analysis, as depicted in Figure S2. The DMC-P123-150 and DMC-P123-200 catalysts displayed a cubic particle shape, while DMC-P123 catalysts calcined at temperatures below 100 °C exhibited a flower-like morphology.[26,29] This morphological shift exhibited a clear correlation with calcination temperature; a transition from amorphous to crystalline in the DMC catalyst's structure was evident with increasing temperature as discussed in the XRD results. These results show a strong correlation between the calcination temperature and the catalyst morphology. Notably, the flower-like structure of the DMC catalyst demonstrated good activity in the copolymerization of PO and $CO_2$.

Figure 2B shows the FT-IR spectra of the DMC-Pure and DMC-P123 catalysts. For all DMC catalysts, an absorption band at 1623 cm$^{-1}$, corresponding to the O−H stretching and deformation vibrations of adsorbed water molecules, was observed.[30] However, for the DMC-P123 catalysts, the distinctive peak attributed to the C≡N stretching vibration shifted to higher wavenumbers (2191−2189 cm$^{-1}$) compared with that for DMC-Pure (2180 cm$^{-1}$), indicating the roles of C≡N$^-$ as a $\sigma$-donor to Co$^{3+}$ and $\pi$-donor to Zn$^{2+}$.[9,31,32] Signals in the range of 2965−2865 cm$^{-1}$, associated with the stretching vibrations of the CH$_3$, CH$_2$, and CH groups in the P123 block copolymer, were observed for all DMC-P123 catalysts.[33,34] Additionally, absorption bands related to the C−O−H and O−H stretching vibrations of P123 appeared between 1323 and 1056 cm$^{-1}$.[35,36] However, as the calcination temperature of the DMC catalyst increased, the intensity of the signals related to P123 decreased and eventually disappeared for the DMC-P123 catalyst calcined at 200 °C, indicating the thermal degradation of P123. Furthermore, for DMC-P123−150 and DMC-P123−200, the other signals were significantly diminished, with only two remaining major peaks corresponding to the C≡N bond and adsorbed water molecules. The XRD and FT-IR results collectively demonstrate the importance of optimizing the calcination temperature of the DMC catalyst to achieve the desired catalytic properties.

Therefore, the catalyst calcined at 100 °C (DMC-P123−100) was selected for the synthesis of PPC polyols in this study owing to its low crystallinity, as evidenced by the XRD patterns, and the presence of the complexing agent, verified by the FT-IR spectra.

The results of the elemental analysis of the DMC-P123 catalysts by ICP-AES are presented in Table 2. The Zn/Co

**Table 2. Physicochemical Properties of the DMC-P123 Catalysts**

| catalyst | elemental composition (wt %) | | Zn/Co mole ratio | BET surface area (m²/g) |
|---|---|---|---|---|
| | Co | Zn | | |
| DMC-P123-60 | 5.88 | 17.93 | 2.7 | 22.0 |
| DMC-P123-80 | 6.64 | 18.41 | 2.5 | 38.5 |
| DMC-P123-100 | 6.71 | 18.72 | 2.5 | 55.2 |
| DMC-P123-150 | 8.66 | 23.04 | 2.4 | 61.6 |
| DMC-P123-200 | 10.68 | 27.37 | 2.3 | 182.8 |

mole ratios ranged from 2.6 to 3.0, indicating the presence of unreacted ZnCl$_2$. ZnCl$_2$ is beneficial for the catalytic performance of the DMC catalyst, as PO monomers are activated by binding to Zn$^{2+}$ sites, thus enhancing their polymerization.[24,37] However, ZnCl$_2$ itself without a DMC catalyst exhibited no activity for this copolymerization.

Table 2 further shows the BET surface areas of DMC-P123-60 to DMC-P123-200, which varied from 22.0 to 182.8 m²/g, depending on the calcination temperature. Calcination involves the removal of volatile organic compounds from the catalyst, resulting in the formation of a highly porous structure that increases the BET surface area. However, there was no relationship between the BET surface area and the copolymerization activity of the catalysts.[22]

The XPS spectra of the DMC-P123 catalysts are presented in Figure S3 and summarized in Table S1. In the expanded Zn 2p XPS spectra shown in Figure S4, all DMC-P123 catalysts exhibited two singlet peaks, regardless of the calcination temperature. This observation suggests that the coordination mode of the complexing agent on the catalyst surface remained unchanged by variations in calcination temperature.[31] On the

other hand, when $ZnCl_2$ and $K_3[Co(CN)_6]_2$ reacted in the presence of the CA (P123), the binding energy of the zinc atom in $ZnCl_2$ (1023.7 eV) shifts to lower values by up to 1.54 eV. This shift in binding energy is attributed to the coordination of oxygen atoms to zinc in $ZnCl_2$.[38] Analyzing the impact of varying catalyst calcination temperatures, the DMC-P123−100 catalyst exhibited the most significant shift in zinc binding energy, indicating strong coordination between Zn and CA. Furthermore, the quantity of coordinated oxygen holds significance, as zinc ions coordinated with oxygen atoms serve as active sites in the PO and $CO_2$ copolymerization mechanism.[39] Comparing the O/Zn values in Table 3 to assess

**Table 3. Surface Compositions and the Atomic Ratio of DMC Catalysts Calcined at Different Temperatures from XPS Analysis**

| Catalyst | Atomic compositions (%) | | | | | | |
|---|---|---|---|---|---|---|---|
| | Zn 2p3 | Co 2p3 | O 1s | N 1s | C 1s | Cl 2p3 | O/Zn |
| DMC-P123-60 | 5.75 | 2.23 | 16.4 | 11.65 | 60.59 | 3.28 | 2.85 |
| DMC-P123-80 | 5.9 | 2.15 | 16.74 | 11.24 | 59.47 | 4.06 | 2.84 |
| DMC-P123-100 | 6 | 2.43 | 17.19 | 12.09 | 59.1 | 3.64 | 2.87 |
| DMC-P123-150 | 6.92 | 2.44 | 16.11 | 12.65 | 57.16 | 4.72 | 2.33 |
| DMC-P123-200 | 7.23 | 2.84 | 11.57 | 15.93 | 57.51 | 4.93 | 1.60 |

the amount of coordinated oxygen, the O/Zn ratio for the DMC-P123−100 catalyst increased to 2.87, while that for the DMC-P123−200 catalyst decreased to 1.60. These results highlight the effective coordination of P123 within the zinc sites of DMC catalysts calcined at a suitable temperature, consistent with the FT-IR results (Figure 2B).

The thermal stability of the DMC catalyst is an essential consideration when determining the optimal calcination temperature and was evaluated by TGA, as shown in Figure 3 and Table 4. The results revealed different weight loss patterns and decomposition temperatures depending on the calcination temperature of the catalyst. DMC-Pure underwent significant weight loss between 40 and 100 °C, primarily due to the loss of water. At 200−350 °C, the weight loss was minimal,

indicating a relatively stable weight. Subsequently, a weight loss of 30.8% was observed at 350−550 °C, indicating the decomposition of cyanide. The residue content ($m_{residue}$) was 56.6%, indicating relatively good heat resistance. The DMC-P123 catalysts exhibited thermal properties different from DMC-Pure. Figure 3B presents the four stages of weight loss observed from the derivative thermogravimetry (DTG) curves. Loss of physically adsorbed water molecules initially occurred at 40−180 °C (first stage),[40] followed by removal of chemically bonded water molecules at 180−320 °C (second stage). The weight loss at 320−370 °C (third stage) was due to the loss of the organic complexing agent, P123,[41] and that at 370−550 °C (fourth stage) was induced by the decomposition of cyanide moieties.[17] The composition (water, P123, and cyanide) and thermal stability of the DMC-P123 catalysts were influenced by the calcination temperature. Highly crystalline DMC-Pure underwent cyanide decomposition at 510 °C, while DMC-P123−60, 80, 100, and 150 decomposed at lower temperatures (410−420 °C). This indicates that a catalyst with a monoclinic structure and lower crystallinity decomposes more easily than that with a cubic structure.[42] Additionally, DMC-P123−200 contained a smaller amount of coordinated P123 (also confirmed by FT-IR spectroscopy; Figure 2B). The TGA results indicated a negative correlation between thermal stability and catalytic activity. Specifically, DMC-P123-60, -80, and -100, which had similarly low $m_{residue}$, exhibited better catalytic performance in the copolymerization of PO and $CO_2$ than DMC-Pure, DMC-P123-150, and DMC-P123-200, which had higher $m_{residue}$ values (Table 4 and Figure 1).

**Effect of Carbonate Content.** DMC-P123-100, which exhibited the highest catalytic activity among the catalysts, was used to synthesize PPC polyols with different carbonate contents. The activity of this catalyst is superior to that of similar experiments conducted using DMC catalysts that have been reported previously. The productivity of the DMC-P123-100 catalyst prepared in this study was 648 g/gcat with a $CO_2$ content of 14.1 wt % while maintaining the reactor pressure at 20 barg. In contrast, DMC-$^t$BuOH-PPG exhibited productivity of 686 g/gcat despite not utilizing $CO_2$.[38] Furthermore, in the case of the $TiO_2$-DMC catalyst, the $CO_2$ content was 9.3 wt % even though the reaction was carried out at 30 bar.[43] The chemical structures of the PPC polyols were investigated by $^1$H NMR spectroscopy, and representative spectra are shown in
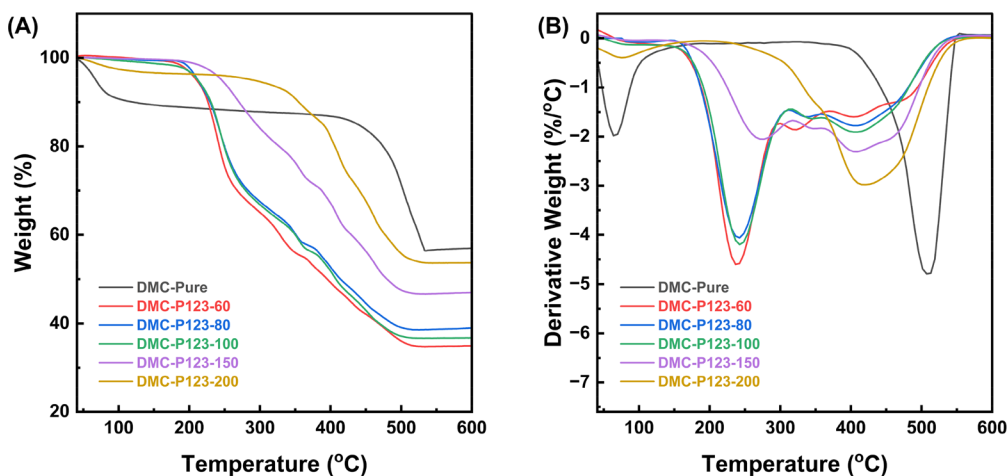


**Figure 3.** (A) TG and (B) DTG curves of the DMC catalysts calcined at different temperatures.

**Table 4. Quantitative Characteristics of Stages in the TG-DTG Curves**

| | mass loss stages (%) | | | | |
| --- | --- | --- | --- | --- | --- |
| catalyst | 40−180 °C | 180−320 °C | 320−370 °C | 370−550 °C | $m_{residue}$ (%) |
| DMC-Pure | 11.24 (40−200 °C) | 1.33 (200−350 °C) | | 30.79 (350−550 °C) | 56.64 |
| DMC-P123−60 | 0.94 | 33.56 | 10.15 | 20.56 | 34.79 |
| DMC-P123−80 | 0.56 | 34.44 | 7.44 | 18.89 | 38.67 |
| DMC-P123−100 | 1.77 | 35.16 | 7.47 | 18.92 | 36.68 |
| DMC-P123−150 | 0.54 | 19.81 | 8.57 | 24.35 | 46.73 |
| DMC-P123−200 | 3.64 (40−200 °C) | 9.97 (200−380 °C) | | 32.75 | 53.64 |

Figure 4. The resonance peak at 5.1 ppm was assigned to the CH group in the carbonate units; those at 1.35 and 1.22 ppm
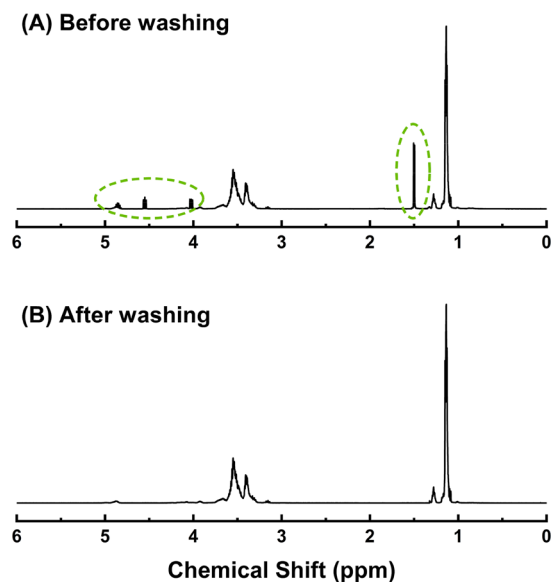


**Figure 4.** $^1$H NMR spectra of PPC polyol-16 (A) before and (B) after washing.

to the CH$_3$ group in the carbonate units and ether linkages, respectively;[1,6,10] and those at 3.3−3.8 ppm to both the CH and CH$_2$ groups in the ether linkages. Furthermore, the formation of the cPC byproduct was confirmed by the appearance of peaks at 4.6, 4.2, and 1.5 ppm in the spectrum obtained before washing. However, after washing, these peaks disappeared (Figure 4B), confirming the successful removal of cPC.

The $W_C$ and $W_{PC}$ values calculated from the integrated peak areas are summarized in Table 5. $W_C$ increased from 0 to 21.0 wt % as the initial pressure of the reactor was raised from 0 to 25 barg. By maintaining the pressure at 20 barg throughout the reaction, a carbonate content of 32.8 wt % was achieved. These results suggest a positive correlation between $W_C$ and the CO$_2$ pressure, demonstrating that the propylene carbonate content of PPC polyol can be effectively controlled by adjusting the CO$_2$ pressure during copolymerization. $W_{PC}$ increased with increasing CO$_2$ pressure, following the same trend as $W_C$. Notably, the amount of polyol product decreased, while $W_{PC}$ increased, with increasing CO$_2$ pressure (Table 5). This is due to the increased number of propagation chains with a terminal zinc carboxylate intermediate (Zn−OOCO−) at higher CO$_2$ pressures. The reduced stability of this intermediate makes it more susceptible to decomposition to cPC.[44,45]

The molecular weight of the polyol decreased with an increasing carbonate content (Table 5). This can be explained

**Table 5. Effect of CO$_2$ Pressure on the Catalytic Activity of DMC-P123-100 in the Copolymerization of PO and CO$_2$**

| $P_{CO2}$ (barg) | polyol product (g) | mol wt (g/mol) | | | $W_C$ (wt %) | $W_{PC}$ (wt %) |
| --- | --- | --- | --- | --- | --- | --- |
| | | $M_n$ | $M_w$ | PDI | | |
| 0 | 160.0 | 4663 | 6192 | 1.3 | | |
| 5 | 143.3 | 4459 | 6777 | 1.5 | 8.2 | 3.4 |
| 10 | 141.5 | 4211 | 7121 | 1.7 | 11.8 | 6.4 |
| 15 | 132.9 | 4183 | 8756 | 2.1 | 16.1 | 9.6 |
| 20 | 132.5 | 3993 | 8063 | 2.0 | 17.1 | 11.4 |
| 25 | 129.9 | 3878 | 9160 | 2.4 | 21.0 | 15.2 |
| m-20[a] | 94.7 | 3043 | 7544 | 2.5 | 32.8 | 24.6 |

[a]Reactor internal pressure maintained at 20 barg during polymerization.

by the previously reported reaction mechanism of the DMC catalyst. The Zn−O bond in the DMC catalyst primarily activates CO$_2$, while unsaturated Zn$^{2+}$ activates PO.[26] Continuous incorporation of the activated PO and CO$_2$ into the Zn−O bonds occurs, followed by a transfer reaction to the initiator (PPG-1000 in this study) and insertion of the PO monomer for propagation.[6] However, continuous CO$_2$ insertion due to excess CO$_2$ disrupts the contact between the PO and the active chain, leading to an unstable structure. Consequently, the molecular weight of the polyol decreases with increasing the CO$_2$ pressure. Moreover, a higher carbonate content results in a higher PDI (up to 2.5 in this study) because of the slow chain transfer reaction between the initiator and active site.

The PPC polyols with different carbonate contents were further characterized by FT-IR spectroscopy (Figure 5). A comparison with the spectrum of PPC polyol-0 ($W_C$ = 0 wt %) revealed the appearance of new peaks at 1742, 1255, and 960 cm$^{-1}$ in the spectra of the other products. These peaks correspond to the stretching vibrations of the C═O and C−O bonds in the carbonate unit in the polyol,[1,21] confirming the successful incorporation of CO$_2$ into the copolymers. Importantly, as $W_C$ increased (Table 5), the intensities of these peaks also increased. Additionally, an absorption peak corresponding to the C−O stretching vibration of the ether linkages was observed at 1085 cm$^{-1}$.[45] The absence of an absorption peak corresponding to the C═O asymmetric vibration at 1800 cm$^{-1}$, along with confirmation from $^1$H NMR data (Figure 4), proved the successful elimination of cPC from the final product.[46]

**Rheological Properties.** Figure 6A depicts the relationship between the viscosity and shear rate of the PPC polyols synthesized using DMC catalysts calcined at temperatures near the optimal temperature of 100 °C. The PPC polyols polymerized using DMC-P123-80, DMC-P123-100, and DMC-P123-150 exhibited similar rheological behavior charac-
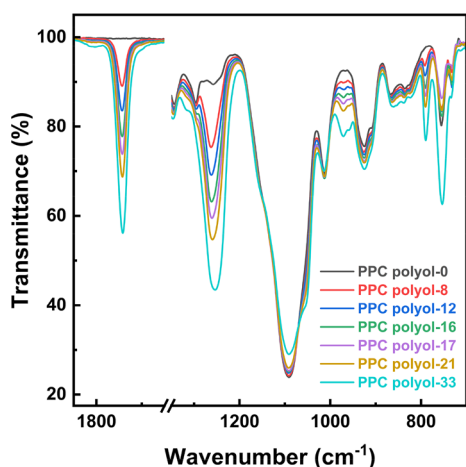
**Figure 5.** FT-IR spectra of PPC polyols with different carbonate contents in the range of 1850−950 cm$^{-1}$ with a break at 1650−1350 cm$^{-1}$.

the hydrogen bond interactions between the electronegative oxygen atoms of the carbonate groups and hydrogen atoms of the terminal hydroxyl groups of PPC polyols. Increasing the $CO_2$ pressure during polymerization increases the number of carbonate groups, thereby increasing the probability of hydrogen bonding between the polyols and resulting in a stronger intermolecular attraction. Because intermolecular interactions play a critical role in determining the viscosity of a liquid,[47,48] variations in intermolecular attraction facilitated by hydrogen bonding contribute to the observed changes in viscosity. Another possible explanation involves the molecular topology of the PPC polyols. The trigonal planar arrangement of the carbon and oxygen atoms in the carbonate group can increase the steric strain and enhance the stiffness of the polyol chain, thereby influencing viscosity. Overall, these findings indicate that the use of the DMC-P123 catalyst enables effective control of the rheological properties of PPC polyols by adjusting the $CO_2$ pressure to modify the propylene carbonate content ($W_C$).

## ■ CONCLUSIONS

In this study, DMC-P123 catalysts, prepared with P123 as the complexing agent, exhibited enhanced catalytic activity, owing to reduced crystallinity and transformation of the crystalline structure from cubic to monoclinic. Specifically, DMC-P123-100 calcined at 100 °C exhibited the highest catalytic performance, owing to its distinct monoclinic phase and a shorter induction period compared to that of the other catalysts. The copolymerization of PO and $CO_2$ using DMC-P123-100 at different $CO_2$ pressures revealed that increasing the carbonate content decreases the molecular weight, broadens the molecular weight distribution, and decreases the polyol productivity. Notably, by controlling the $CO_2$ pressure, a propylene carbonate content of up to 32.8 wt % was obtained, which is higher than those achieved in previous studies. The rheological analysis emphasized the critical role of determining the favorable calcination temperature in successfully synthesizing PPC polyols with desirable properties. Furthermore, increasing the $CO_2$ pressure increased the carbonate content of the PPC polyols. This resulted in enhanced intermolecular attraction and a higher probability of hydrogen bonding between polyol chains, leading to increased
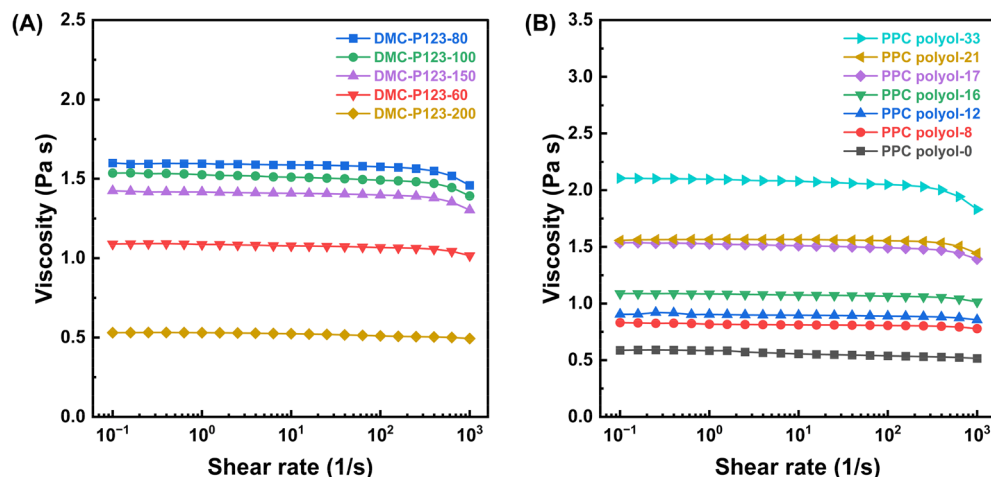
terized by comparable viscosities. Notably, the PPC polyols demonstrate remarkable viscosity stability across a broad spectrum of shear rates. This characteristic arises from the low molecular weight of the polyol molecules, which facilitates relaxation even under high shear rate conditions. The analogous viscosity and shear-thinning behavior indicate the successful synthesis of similar PPC polyols using these three catalysts. However, the PPC polyols polymerized by using DMC-P123-60 and DMC-P123-200 had significantly lower viscosities without clear shear-thinning behavior at large shear rates. The absence of shear-thinning behavior indicates that the PPC polyol polymerized using DMC-P123-200 had much smaller molecular weights than those polymerized using other DMC-P123 catalysts. This finding is consistent with the results of the GPC analysis (Table 1), reinforcing the importance of optimal calcination conditions.

Figure 6B illustrates the viscosity of PPC polyols polymerized at varying $CO_2$ pressures as a function of the shear rate. Notably, polyols polymerized at higher $CO_2$ pressures had significantly higher viscosities and demonstrated clear shear-thinning behavior. A possible explanation for the positive correlation between the $CO_2$ pressure and viscosity is



**Figure 6.** Flow curves of (A) PPC polyols synthesized by using DMC-P123 catalysts calcined at various temperatures and (B) PPC polyols with different carbonate contents.

viscosity. These findings on $CO_2$-based polyols afford PU products with chemical and rheological properties that enable effective $CO_2$ utilization and contribute to reducing the carbon footprint in chemical synthesis.

## ■ ASSOCIATED CONTENT

### ⓈⒾ Supporting Information

The Supporting Information is available free of charge at https://pubs.acs.org/doi/10.1021/acsomega.3c04765.

    (PDF)

## ■ AUTHOR INFORMATION

### Corresponding Author

    **Joon Hyun Baik** − *Department of Chemical and Biological Engineering and Institute of Advanced Materials and Systems, Sookmyung Women's University, Seoul 04310, Republic of Korea;* ⓞ orcid.org/0000-0001-9967-5080; Phone: +82-2-2077-7853; Email: joonhyun@sookmyung.ac.kr

### Authors

    **Harin Kim** − *Department of Chemical and Biological Engineering, Sookmyung Women's University, Seoul 04310, Republic of Korea*

    **Hyo-Jeong Lee** − *Department of Chemical and Biological Engineering, Sookmyung Women's University, Seoul 04310, Republic of Korea*

    **Jiwon Hwang** − *Department of Chemical and Biological Engineering, Sookmyung Women's University, Seoul 04310, Republic of Korea*

    **Su Min Jung** − *Department of Chemical and Biological Engineering, Sookmyung Women's University, Seoul 04310, Republic of Korea*

    **Jun Dong Park** − *Department of Chemical and Biological Engineering and Institute of Advanced Materials and Systems, Sookmyung Women's University, Seoul 04310, Republic of Korea*

Complete contact information is available at:
https://pubs.acs.org/10.1021/acsomega.3c04765

### Notes

The authors declare no competing financial interest.

## ■ REFERENCES

(1) Meng, Q.; Cheng, R.; Li, J.; Wang, T.; Liu, B. Copolymerization of $CO_2$ and Propylene Oxide Using ZnGA/DMC Composite Catalyst for High Molecular Weight Poly(propylene carbonate). *J. $CO_2$ Util.* **2016**, *16*, 86−96.

(2) Langanke, J.; Wolf, A.; Hofmann, J.; Böhm, K.; Subhani, M. A.; Müller, T. E.; Leitner, W.; Gürtler, C. Carbon Dioxide ($CO_2$) as Sustainable Feedstock for Polyurethane Production. *Green Chem.* **2014**, *16*, 1865−1870.

(3) Alagi, P.; Ghorpade, R.; Choi, Y. J.; Patil, U.; Kim, I.; Baik, J. H.; Hong, S. C. Carbon Dioxide-Based Polyols as Sustainable Feedstock of Thermoplastic Polyurethane for Corrosion-Resistant Metal Coating. *ACS Sustain. Chem. Eng.* **2017**, *5*, 3871−3881.

(4) Carvalho, K.; Alves, R. M. B.; Kulay, L. Environmental Performance of Alternative Green Polyol Synthesis Routes: A Proposal for Improvement. *Processes* **2021**, *9*, 1122.

(5) Deacy, A. C.; Kilpatrick, A. F. R.; Regoutz, A.; Williams, C. K. Understanding Metal Synergy in Heterodinuclear Catalysts for the Copolymerization of $CO_2$ and Epoxides. *Nat. Chem.* **2020**, *12*, 372−380.

(6) Jang, J. H.; Ha, J. H.; Kim, I.; Baik, J. H.; Hong, S. C. Facile Room-Temperature Preparation of Flexible Polyurethane Foams from Carbon Dioxide Based Poly(ether carbonate) Polyols with a Reduced Generation of Acetaldehyde. *ACS Omega* **2019**, *4*, 7944−7952.

(7) von der Assen, N.; Bardow, A. Life Cycle Assessment of Polyols for Polyurethane Production Using $CO_2$ as Feedstock: Insights from an Industrial Case Study. *Green Chem.* **2014**, *16*, 3272−3280.

(8) Liu, S.; Miao, Y.; Qiao, L.; Qin, Y.; Wang, X.; Chen, X.; Wang, F. Controllable Synthesis of a Narrow Polydispersity $CO_2$-Based Oligo(Carbonate-Ether) Tetraol. *Polym. Chem.* **2015**, *6*, 7580−7585.

(9) Tran, C. H.; Kim, S. A.; Moon, Y.; Lee, Y.; Ryu, H. M.; Baik, J. H.; Hong, S. C.; Kim, I. Effect of Dicarbonyl Complexing Agents on Double Metal Cyanide Catalysts toward Copolymerization of $CO_2$ and Propylene Oxide. *Catal. Today* **2021**, *375*, 335−342.

(10) Lee, D. H.; Ha, J. H.; Kim, I.; Baik, J. H.; Hong, S. C. Carbon Dioxide Based Poly(ether carbonate) Polyol in Bi-polyol Mixtures for Rigid Polyurethane Foams. *J. Polym. Environ.* **2020**, *28*, 1160−1168.

(11) Marquez, C.; Rivera-Torrente, M.; Paalanen, P. P.; Weckhuysen, B. M.; Cirujano, F. G.; De Vos, D.; De Baerdemaeker, T. Increasing the Availability of Active Sites in Zn-Co Double Metal Cyanides by Dispersion onto a $SiO_2$ Support. *J. Catal.* **2017**, *354*, 92−99.

(12) Peeters, A.; Valvekens, P.; Ameloot, R.; Sankar, G.; Kirschhock, C. E. A.; De Vos, D. E. Zn−Co Double Metal Cyanides as Heterogeneous Catalysts for Hydroamination: A Structure−Activity Relationship. *ACS Catal.* **2013**, *3*, 597−607.

(13) Oh, H. J.; Ko, Y. S. Effect of Polymerization Conditions on the Polymer Properties of $CO_2$-Cyclohexene Oxide Copolymer Prepared by Double Metal Cyanide Catalyst. *J. Ind. Eng. Chem.* **2013**, *19*, 1939−1943.

(14) Lee, I. K.; Ha, J. Y.; Cao, C.; Park, D.-W.; Ha, C.-S.; Kim, I. Effect of Complexing Agents of Double Metal Cyanide Catalyst on the Copolymerizations of Cyclohexene Oxide and Carbon Dioxide. *Catal. Today* **2009**, *148*, 389−397.

(15) Stahl, S.-F.; Luinstra, G. A. DMC-Mediated Copolymerization of $CO_2$ and PO—Mechanistic Aspects Derived from Feed and Polymer Composition. *Catalysts* **2020**, *10*, 1066.

(16) Li, X. H.; Meng, Y. Z.; Zhu, Q.; Tjong, S. C. Thermal Decomposition Characteristics of Poly(propylene carbonate) Using TG/IR and Py-GC/MS Techniques. *Polym. Degrad. Stab.* **2003**, *81*, 157−165.

(17) Jadhav, A. R.; Bandal, H. A.; Kim, H. Synthesis of Substituted Amines: Catalytic Reductive Amination of Carbonyl Compounds Using Lewis Acid Zn−Co-Double Metal Cyanide/Polymethylhydrosiloxane. *Chem. Eng. J.* **2016**, *295*, 376−383.

(18) Marquez, C.; Simonov, A.; Wharmby, M. T.; Van Goethem, C.; Vankelecom, I.; Bueken, B.; Krajnc, A.; Mali, G.; De Vos, D.; De Baerdemaeker, T. Layered $Zn_2[Co(CN)_6](CH_3COO)$ Double Metal Cyanide: A Two-Dimensional DMC Phase with Excellent Catalytic Performance. *Chem. Sci.* **2019**, *10*, 4868−4875.

(19) Kopczyńska, P.; Datta, J. Single-Phase Product Obtained via Crude Glycerine Depolymerisation of Polyurethane Elastomer: Structure Characterisation and Rheological Behaviour. *Polym. Int.* **2016**, *65*, 946−954.

(20) Głowińska, E.; Datta, J. A Mathematical Model of Rheological Behavior of Novel Bio-Based Isocyanate-Terminated Polyurethane Prepolymers. *Ind. Crops Prod.* **2014**, *60*, 123−129.

(21) Chen, S.; Xiao, Z.; Ma, M. Copolymerization of Carbon Dioxide and Epoxides with a Novel Effective Zn−Ni Double-Metal Cyanide Complex. *J. Appl. Polym. Sci.* **2008**, *107*, 3871−3877.

(22) Sebastian, J.; Srinivas, D. Factors Influencing Catalytic Activity of Co−Zn Double-Metal Cyanide Complexes for Alternating Polymerization of Epoxides and $CO_2$. *Appl. Catal., A* **2015**, *506*, 163−172.

(23) Mullica, D. F.; Milligan, W. O.; Beall, G. W.; Reeves, W. L. Crystal Structure of $Zn_3[Co(CN)_6]_2.12H_2O$. *Acta Crystallogr. Sect. B: Struct. Crystallogr. Cryst. Chem.* **1978**, *B34*, 3558−3561.

(24) Marquez, C.; Corbet, M.; Smolders, S.; Marion, P.; De Vos, D. Double Metal Cyanides as Heterogeneous Lewis Acid Catalysts for Nitrile Synthesis via Acid-Nitrile Exchange Reactions. *Chem. Commun.* **2019**, *55*, 12984−12987.

(25) Dienes, Y.; Leitner, W.; Müller, M. G. J.; Offermans, W. K.; Reier, T.; Reinholdt, A.; Weirich, T. E.; Müller, T. E. Hybrid Sol−Gel Double Metal Cyanide Catalysts for the Copolymerisation of Styrene Oxide and $CO_2$. *Green Chem.* **2012**, *14*, 1168−1177.

(26) An, N.; Li, Q.; Yin, N.; Kang, M.; Wang, J. Effects of Addition Mode on Zn−Co Double Metal Cyanide Catalyst for Synthesis of Oligo(propylene-carbonate) Diols. *Appl. Organomet. Chem.* **2018**, *32*, No. e4509.

(27) Zhang, W.; Lin, Q.; Cheng, Y.; Lu, L.; Lin, B.; Pan, L.; Xu, N. Double Metal Cyanide Complexes Synthesized by Solvent-Free Grinding Method for Copolymerization of $CO_2$ and Propylene Oxide. *J. Appl. Polym. Sci.* **2012**, *123*, 977−985.

(28) Tran, C. H.; Pham, L. T. T.; Jang, H. B.; Kim, S. A.; Kim, I. Effect of $\alpha$-, $\beta$-, $\gamma$-, and $\delta$-Dicarbonyl Complexing Agents on the Double Metal Cyanide-Catalyzed Ring-Opening Polymerization of Propylene Oxide. *Catal. Today* **2021**, *375*, 429−440.

(29) Yang, P.; Yu, M.; Fu, J.; Wang, L. Synthesis and Microwave Absorption Properties of Hierarchical Fe Micro-Sphere Assembly by Nano-Plates. *J. Alloys Compd.* **2017**, *721*, 449−455.

(30) Teoh, L. G.; Shieh, J.; Lai, W. H.; Hung, I. M.; Hon, M. H. Structure and Optical Properties of Mesoporous Tungsten Oxide. *J. Alloys Compd.* **2005**, *396*, 251−254.

(31) Tran, C. H.; Pham, L. T. T.; Lee, Y.; Jang, H. B.; Kim, S.; Kim, I. Mechanistic Insights on Zn(II)−Co(III) Double Metal Cyanide-Catalyzed Ring-Opening Polymerization of Epoxides. *J. Catal.* **2019**, *372*, 86−102.

(32) Yang, L. M.; Lv, P. M.; Yuan, Z. H.; Luo, W.; Wang, Z. M.; Li, H. W. Promoting Effect of Metal Promoters on Fe(II)-Zn-Based Double Metal Cyanide Complex Catalysts for Biodiesel Synthesis. *Adv. Mater. Res.* **2011**, *236−238*, 3041−3045.

(33) Mgwetyana, U.; Makhatha, M. E.; Mamo, M.; Ndungu, P. Synthesis and Characterization of Mesoporous Titania Using a Synthetic (Pluronic P123) and a Natural (Gum Arabic) Templating Agent. *Mater. Today: Proc.* **2018**, *5*, 10585−10591.

(34) Cao, S.-W.; Zhu, Y.-J.; Wu, J.; Wang, K.-W.; Tang, Q.-L. Preparation and Sustained-Release Property of Triblock Copolymer/ Calcium Phosphate Nanocomposite as Nanocarrier for Hydrophobic Drug. *Nanoscale Res. Lett.* **2010**, *5*, 781.

(35) Shameli, K.; Bin Ahmad, M.; Jazayeri, S. D.; Sedaghat, S.; Shabanzadeh, P.; Jahangirian, H.; Mahdavi, M.; Abdollahi, Y. Synthesis and Characterization of Polyethylene Glycol Mediated Silver Nanoparticles by the Green Method. *Int. J. Mol. Sci.* **2012**, *13*, 6639−6650.

(36) Song, H.-M.; Zink, J. I. Ag(I)-Mediated Self-Assembly of Anisotropic Rods and Plates in the Surfactant Mixture of CTAB and Pluronics. *RSC Adv.* **2019**, *9*, 4380−4389.

(37) Lee, S. H.; Lee, I. K.; Ha, J. Y.; Jo, J. K.; Park, I.; Ha, C.-S.; Suh, H.; Kim, I. Tuning of the Activity and Induction Period of the Polymerization of Propylene Oxide Catalyzed by Double Metal Cyanide Complexes Bearing $\beta$-Alkoxy Alcohols as Complexing Agents. *Ind. Eng. Chem. Res.* **2010**, *49*, 4107−4116.

(38) Kim, I.; Ahn, J.-T.; Ha, C. S.; Yang, C. S.; Park, I. Polymerization of Propylene Oxide by Using Double Metal Cyanide Catalysts and the Application to Polyurethane Elastomer. *Polymer* **2003**, *44*, 3417−3428.

(39) Almora-Barrios, N.; Pogodin, S.; Bellarosa, L.; García-Melchor, M.; Revilla-López, G.; García-Ratés, M.; Vázquez-García, A. B.; Hernández-Ariznavarreta, P.; López, N. Structure, Activity, and Deactivation Mechanisms in Double Metal Cyanide Catalysts for the Production of Polyols. *ChemCatChem.* **2015**, *7*, 928−935.

(40) Tran, C.-H.; Lee, M.-W.; Lee, S.-J.; Choi, J.-H.; Lee, E.-G.; Choi, H.-K.; Kim, I. Highly Active Heterogeneous Double Metal Cyanide Catalysts for Ring-Opening Polymerization of Cyclic Monomers. *Polymers* **2022**, *14*, 2507.

(41) Mirtaheri, B.; Shokouhimehr, M.; Beitollahi, A. Synthesis of Mesoporous Tungsten Oxide by Template-Assisted Sol−Gel Method and its Photocatalytic Degradation Activity. *J. Sol-Gel Sci. Technol.* **2017**, *82*, 148−156.

(42) Sebastian, J.; Srinivas, D. Effects of Method of Preparation on Catalytic Activity of Co−Zn Double-Metal Cyanide Catalysts for Copolymerization of $CO_2$ and Epoxide. *Appl. Catal., A* **2014**, *482*, 300−308.

(43) Subhani, M. A.; Gürtler, C.; Leitner, W.; Müller, T. E. Nanoparticulate $TiO_2$-Supported Double Metal Cyanide Catalyst for the Copolymerization of $CO_2$ with Propylene Oxide. *Eur. J. Inorg. Chem.* **2016**, *2016*, 1944−1949.

(44) Luinstra, G. A.; Haas, G. R.; Molnar, F.; Bernhart, V.; Eberhardt, R.; Rieger, B. On the Formation of Aliphatic Polycarbonates from Epoxides with Chromium(III) and Aluminum-(III) Metal−Salen Complexes. *Chem.—Eur. J.* **2005**, *11*, 6298−6314.

(45) Gao, Y.; Qin, Y.; Zhao, X.; Wang, F.; Wang, X. Selective Synthesis of Oligo(carbonate-ether) Diols from Copolymerization of $CO_2$ and Propylene Oxide under Zinc-Cobalt Double Metal Cyanide Complex. *J. Polym. Res.* **2012**, *19*, No. 9878.

(46) Luo, L.; Wang, W.-Z.; Wang, L.; Li, L.-L.; Zhang, Y.-L.; Zhao, S.-D. Copolymerization of $CO_2$, Propylene Oxide, and Itaconic Anhydride with Double Metal Cyanide Complex Catalyst to Form Crosslinked Polypropylene Carbonate. *e-Polym.* **2021**, *21*, 854−868.

(47) Hirschfelder, J. O.; Curtiss, C. F.; Bird, R. B. *Molecular Theory of Gases and Liquids*; John Wiley and Sons, Inc.: New York, 1964.

(48) Bird, R. B.; Stewart, W. E.; Lightfoot, E. N. *Transport Phenomena*, 2nd ed.; John Wiley and Sons, Inc.: New York, 2007.